Optics & Laser Technology 90 (2017) 102–108

Contents lists available at ScienceDirect

Optics & Laser Technology

journal homepage: www.elsevier.com/locate/optlastec

Photoluminescent colloidal Cu@C-NPs suspensions synthesized by LASL

D. Reyes-Contreras[a,*], M.A. González-Aguilar[b], M.A. Camacho-López[c], E. Vigueras-Santiago[d], M. Camacho-López[d,*]

[a] Facultad de Ciencias, Universidad Autónoma del Estado de México, Campus El Cerrillo, Piedras Blancas, Carretera Toluca - Ixtlahuaca Kilómetro 15.5, Edo. de México C.P. 50200, México
[b] Facultad de Química, Universidad Autónoma del Estado de México, Paseo Colon esquina con Paseo Tollocan s/n, Toluca C.P. 50120, México
[c] Laboratorio de Fotomedicina, Biofotónica y Espectroscopía Láser de Pulsos Ultracortos, Facultad de Medicina, Universidad Autónoma del Estado de México, Jesús Carranza y Paseo Tollocan s/n, Toluca C.P. 50120, México
[d] Laboratorio de Investigación y Desarrollo de Materiales Avanzados, Facultad de Química, Universidad Autónoma del Estado de México, Campus Rosedal, Km 14.5 Carretera Toluca-Atlacomulco, San Cayetano de Morelos, Toluca C.P. 50925, México

ARTICLE INFO

Keywords:
Laser ablation
Cu@C-NPs
Light emission

ABSTRACT

In this work we report the synthesis of photoluminescent carbon-coated copper nanoparticles (Cu@C-NPs) based colloidal suspensions, using the laser ablation of solids in liquids technique (LASL). LASL experiments were carried out by ablating a Cu solid target immersed in acetone as the liquid medium with ns-laser pulses (1064 nm) of a Nd-YAG laser. In all experiments the per pulse laser fluence and the repetition rate frequency were kept constant and the ablation time was varied. The as obtained Cu@C-NPs suspensions were optically characterized with absorption and photoluminescence spectroscopies. Raman spectroscopy was used to give evidence of the carbon shell deposited around the Cu NPs. TEM results showed that 10 nm spheroids Cu@C-NPs were obtained. The as obtained Cu@C-NPs suspensions displayed out a PL emission band similar to that for carbon nanoparticles suspensions obtained by the same technique. We have found that the blue-green PL emission band intensity is mainly dependent on the ablation and aging time of the samples. The Cu@C-NPs-based colloidal suspensions can be proposed as multifunctional due to its absorbance and emission properties.

1. Introduction

One of the key benefits of a material in the nanoscale is that its properties considerably differs from the bulk material of the same composition, feature which can be easily altered by varying its size, shape or chemical environment, allowing the possibility to have nanomaterials with well-defined properties for specific applications [1–3]. Nanomaterials of almost any material can be produced i.e., metallic, semiconductors, ceramics and among; and their chemical, physical and optical properties can generally be controlled by the route of synthesis used [4,5], either during or after by a post-synthesis treatment, a surface passivation, for example. In order to tune the properties of nanomaterials, numerous chemical, physical and biological routes of synthesis have been implemented during the past decades [6–8]. An increasing route of synthesis for the production of nanomaterials is the physical method termed laser ablation of solid targets in liquid media (LASL). The increase of its use is mainly because this technique of synthesis is considered as chemically clean (green), simple, versatile and fast; and because through it, nanomaterials from almost whatever bulk material can be obtained [5,6,9,10]. It is necessary to point it out that through the LASL route, different experimental parameters as laser fluence, pulse duration, irradiation time, and among, can be modified in order to have a reasonable control of the nanoparticle size [5], however the grow mechanism of nanoparticles through this technique is very chaotic and the complete information for the perfect control of nanoparticle sizes is still missing. The main goal of the present work is to use LASL route to produce copper-based photoluminiscent nanoparticles.

Copper based-metallic nanomaterials, termed copper nanoparticles (Cu-NPs) have been attractive in different areas by virtue of their useful properties such as the good thermal and electrical conductivity at a much lower cost than silver or gold. Due to its plasmon surface resonance, copper nanoparticles exhibit enhanced nonlinear optical properties, which can result in many applications in optical devices and nonlinear optical materials [11,12]. Due to its potential applications, several routes of synthesis have been implemented for the production of Cu-NPs [11–17]. Only to cite some of them, it can be referred the chemical reduction of copper sulfate method [11], photochemical synthesis [13], laser ablation in liquids [14–17], biological routes [18], and among. It has also been reported the synthesis of small

* Corresponding authors.
E-mail addresses: dreyes.fc@gmail.com (D. Reyes-Contreras), mramanmarco@gmail.com (M. Camacho-López).

http://dx.doi.org/10.1016/j.optlastec.2016.11.004
Received 15 June 2016; Accepted 8 November 2016

fluorescent atomic copper clusters via electrochemical synthesis [19]. The synthesis of copper/copper oxide nanoparticles through solution plasma [20] or via Gram-negative bacterium [21] and the production of electrically conducting copper iodide (CuI) nanoparticles synthesized at room temperature via chemical routes have also been reported [22]. In particular, the production of copper-based nanoparticles using the above mentioned LASL technique requires times of synthesis as short as 100 s [16], which is very short compared with the typical 2–3 h for the chemical routes [12]. Inkjet-printed electronics [12], SERS technique [14], as antibacterial activity agents [18], or optoelectronic applications [22], are only some of the specifics applications of Cu-NPs reported.

Beside of the close-pure Cu-NPs, it has interestingly been reported the synthesis of copper nanoparticles covered with carbon, which have mainly been designed in order to protect the Cu-NPs to the agglomeration phenomena, or to prevent the unwanted degradation phenomena or oxidation, which impacts on its applications. With the aim to have a better understanding and control of the carbon-shell covering the copper-core, the production of carbon-coated copper nanoparticles (Cu@C-NPs) have been possible performing different route of synthesis. To cite some examples, these are synthesized using flame spray synthesis [23], solid-state reduction reactions [24], by detonation decomposition of Cu ions [25], in ionic liquid under microwave heating [26], using hydrothermal methods [27], laser ablation [28,29] and among. Cu-NPs encapsulated in multi-shell carbon cages using Cu-phthalocyanine as precursor material [30] or by multi-layer graphene through metal-organic chemical vapor deposition method [31] or reducing flame synthesis [32], have also been reported. The prevention of the undesired degradation phenomena was also reached by incorporating linear carbon chains [33] containing *sp* hybridization either as alternating triple and single bonds (polyynes). The benefits of the carbon-shell on a copper-core on its applications have been exemplified, indicating that the carbon shell prevents the oxidation, which allows the possibility to use these as temperature or pressure sensors completely exposed to air [23], being also suitable to replacing the expensive noble metal nanoparticles utilized in the conductive inks [30]. Another advantage is due to the carbonaceous shells, preventing the oxidation and aggregation of metal copper, was proposed to be useful to improve the catalytic performance of copper nanostructures [27]. Multifunctional optical applications due to its absorbance and fluorescence properties, like as biomedical, sensor and lubricant ones have been proposed for Cu@C-NPs [28,29,34,35]. It is necessary to point it out that agglomeration can be prevented by adding dispersant or surfactant agents to the solution after its synthesis, however when LASL technique is used, this effect can be reached after some minutes [27,36].

Motivated on the potential applications of copper-core carbon-shell (Cu@C-NPs) nanoparticles, the aims of this paper are focused to report on the one hand, its synthesis using LASL technique, considered as a simple and versatile route; on the other hand show its photoluminescent response and its correlation with the carbon-shell presence. To obtain the Cu@C-NPs, the ablation of copper bulk immersed in acetone was performed at different ablation times. The effect of the ablation time and aging time on the optical properties of the as-well prepared copper suspensions was analyzed, concluding that Cu@C-NPs are formed and the carbon shell is the responsible for the photoluminescence.

2. Experimental

2.1. Synthesis of colloidal Cu@C-NPs in acetone

Colloidal Cu@C-NPs suspensions were obtained using the laser ablation of solids in liquids technique (LASL). The ablation experiments were carried out as is illustrated in Fig. 1A. A copper disk (2.54 cm diameter×0.635 cm long, 99.999% pure, Kurt J. Lesker Co.)

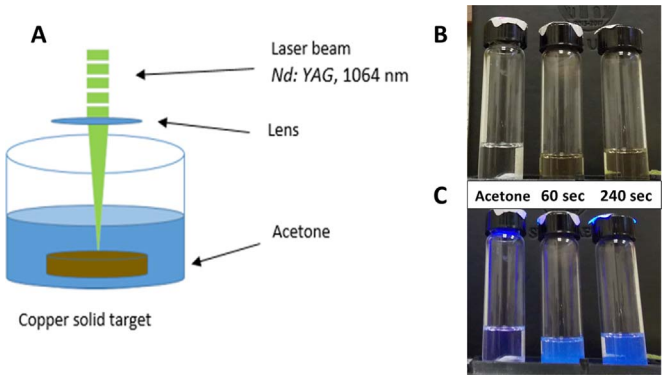

Fig. 1. A-Experimental setup for the Cu@C-NPs synthesis and appearance of the Cu@C-NPs suspensions under white (B) or UV (C) light illumination for different irradiation times and pure acetone. (For interpretation of the references to color in this figure, the reader is referred to the web version of this article.)

was the solid target, which was immersed in 10 ml of pure acetone (*Sigma- Aldrich Co.*), using a glass vessel of 20 ml. By focusing laser pulses (30 mJ per pulse) on the surface of the copper disk by means of a 135 mm focal length lens, the ablation was initiated; the copper disk was manually moved to prevent ablation in the same place, which could change the focus conditions. It is necessary to indicate that the laser beam was not exactly focused on the copper surface; the spot beam have 0.125 cm^2 area (0.2 cm diameter), which is reduced to 0.005 cm^2 area (0.04 cm diameter), giving a laser fluence, according to the power per pulse, 5 J/cm^2. A pulsed Nd:YAG laser (*Minilite II, Continuum*) emitting at 1064 nm and operated at 15 Hz of repetition rate was used in all experiments. Samples for irradiation times of 30, 60, 120, 180, 240 and 300 s (sec) were prepared. Even when through LASL technique many experimental parameters can be tuned in order to control the final properties of the prepared nanoparticles [5], the goal of this study is to elucidate the effect of the irradiation time on the produced copper nanoparticles when keeping constant the solvent, repetition rate frequency, laser fluence and wavelength used for the synthesis. Based on our experimental experience related with LASL technique, flammable solvents as acetone could flame during its interaction with the laser pulses, however it was found to occur when the level of the solvent is slightly above to the target or when the laser beam interacting with the target produces small drops; both possibilities were not present in the LASL experiment reported here, ignition of the acetone was not observed.

Fig. 1B and C shows optical images of the samples under white light and UV (370 nm) illumination, respectively. For comparison purposes, acetone was also included in the picture. In Fig. 1B one can observe a brownish coloration in the liquid similar (samples obtained at 60 and 240 s of ablation time) to that observed in the carbon nanoparticles suspension obtained by LALS from a carbon target immersed in acetone under the same laser parameters previously reported by our group [37]. In Fig. 1C blue photoluminescence is observed in samples illuminated with a UV (370 nm) lamp (pictures were taken after 30 days of the synthesis). The photoluminescence observed in these copper nanoparticles in acetone is similar to that observed in the carbon nanoparticles suspensions in the same solvent reported by our group [37,38].

2.2. Optical and structural characterization

The optical features of the as-obtained Cu@C-NPs and carbon suspensions were investigated by using absorption and photoluminescence spectroscopies. Optical absorption spectra of the suspensions were taken using a double beam spectrophotometer (Perkin-Elmer, Lambda 650) from 320 to 900 nm. A quartz cuvette with an optical path length of 10 mm was used for the optical characterization. The

photoluminescence (PL) spectra were taken using a spectrofluorometer (Jobin-Yvon-Horiba, Fluoromax-p), exciting the samples at 369 nm. The PL spectrum of the quartz cell filled with pure acetone was also recorded for the sake of reference. The excitation and emission spectra of all samples were then collected. All the experiments were performed at environmental conditions (25 °C and 1 atm pressure). Raman characterization of the Cu@C NPs was performed in a microRaman (LabRama HR-800 of Jobin-Yvon-Horiba) system equipped with a red (632.8 nm) He–Ne laser and an optical microscope (Olympus, BX-41). An objective lens of 50X was used to focus down the laser beam, with 0.005 mW laser power on the sample. For Raman analysis, the Cu@C nanoparticles sample was prepared at room temperature by dropping 2.5 ml (~50 drops) of the colloidal Cu nanoparticles suspension on a glass slide. The structural characterization was carried out in a transmission electron microscope (JEOL 2010) with an accelerating voltage of 200 kV. TEM images acquisition was performed in samples prepared by the evaporation at room temperature of a drop of the colloidal Cu@C NPs suspension on the grid.

3. Results and discussion

3.1. SPR of Cu@C NPs in acetone

Fig. 2 shows the absorption spectra for the colloidal Cu@C-NPs samples obtained at different ablation times and measured immediately after its synthesis (2-A), called 0 days, and 30 days (2-B) from their preparation. The absorption band located at 584 nm corresponds to the surface plasmon resonance (SPR) for copper nanoparticles. This is in good agreement with the SPR absorption band position reported between 574 and 581 nm [16,17] and 588 nm [14] for Cu-NPs synthesized in acetone by using the LASL technique; differences are attributed to the different experimental conditions. This absorption band is observed for samples synthesized during 30 s of ablation time and longer. It is clear to observe from 2-A and 2-B that the intensity of the absorption band increases when increasing the ablation time, which is related with the increment of nanoparticles concentration obtained. Even when no quantitative measurements of the Cu-NPs concentration were performed, this increase in the absorbance intensity is an indicative that the copper nanoparticles concentration increment in the colloidal suspension [31]. Hence, the copper nanoparticles concentration can be controlled by means of the ablation time. It is important to point it out that the SPR absorption band position is not significantly dependent on neither the copper nanoparticles concentration (ablation time [31]) nor the time after synthesis; blue or red-shifts of around 3 nm were observed. The spectral position and the SPR absorption band feature indicates that the Cu@C-NPs are spherical and highly monodisperse [39]. The effect of the ablation time on the size and shape of the Cu@C-NPs was not deeply investigated: however it has been previously reported that the size of similar nanoparticles decreases when increasing the laser fluence [16]. In this study, Z-potential analysis to predict and control the stability of the colloidal suspensions was not performed because it was easily observed with naked eyes that in a period of 8 months the as obtained colloidal Cu@C-NPs suspensions presented high stability in terms of precipitation. The stability of copper nanoparticles obtained using the same route was previously reported after 10 months from its synthesis in acetone, being completely different when the synthesis is carried out in deionized water [17].

Fig. 2C shows the absorption intensity measured at 369 nm and at 584 nm (SPR) as a function of the ablation time measured 0 days (squares) and 30 days (triangles) after their synthesis. On the one hand, it can be seen that for the absorption band at 369 nm (wavelength was selected due to the posterior photoluminescence analysis) not only the absorbance increases as a function of ablation

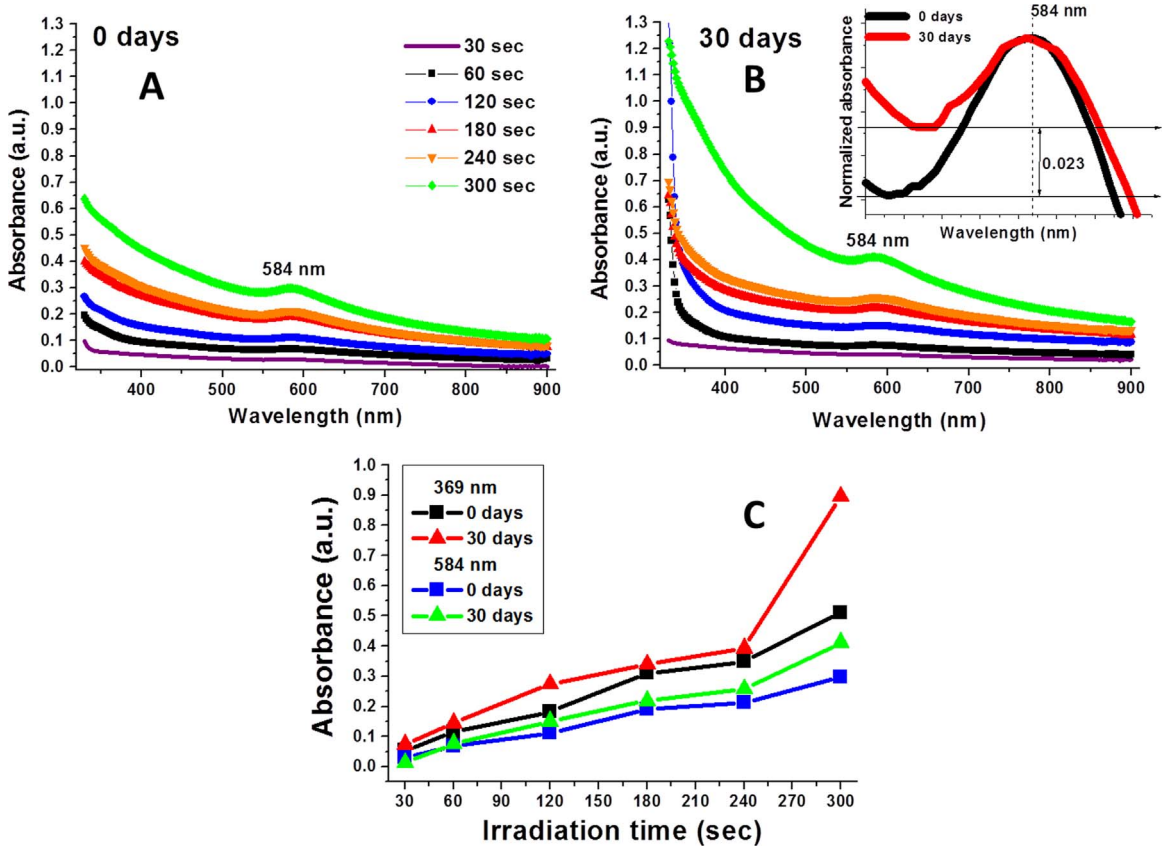

Fig. 2. Absorbance spectra of the Cu@C-NPs immediately (A) after its synthesis (0 days) and 30 days (B) from its synthesis. C - Maximum Absorbance recorded for 369 1 nm for each irradiation time at the times for A, B figures.

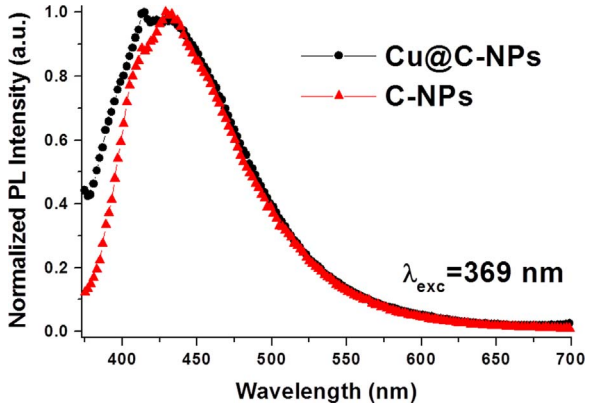

Fig. 3. Normalized PL emission of the Cu@C-NPs (black circles) and the C-NPs (red triangles), both in acetone and under 120 s of ablation time. (For interpretation of the references to color in this figure legend, the reader is referred to the web version of this article.)

time, but also as a function of the aging time, samples aged for 30 days are more absorbents than those aged during 0 days for the same time of synthesis. The increase in the absorption intensity is mainly observed in the UV-blue interval from 330 to 450 nm, this contribution is mostly attributed to the presence of carbon in the Cu@C-NPs. In a previous work, we reported the absorption spectra for carbon nanoparticles in acetone, showing that the absorbance at 369 nm increases as the carbon nanoparticles concentration increases [37], which is in completely agree with the observation reported here. On the other hand, in Fig. 2C the absorbance of the SPR band as a function of the ablation and aging time is also presented: while for the aging time the increase is of 28% (3.4 times lower than that with ablation time), the increase of its intensity due to the ablation time is of 96%.

The inset in Fig. 2B is the normalized absorbance of the SPR band located at 584 nm, 0 and 30 days after its synthesis (aging time); from the inset, it can be seen that its peak position is not changing; however the SPR band for the sample aged 0 days is more intense (0.023) and less broader than that aged for 30 days. This effect can be associated with the original purity of the copper nanoparticles, which turn to be inhomogeneous due to the interaction with the solvent and products from the ablation, beside of the presence of carbon on the copper nanoparticles, which modify the absorbance of the colloidal suspension. While for Cu-NPs synthesized in acetone and aged 10 h a peak shift of 11 nm of the SPR band including a decrease in the intensity was reported [17], for Cu-NPs synthesized in ethanol and aged 7 days, a minuscule peak shift of the SPR band was observed with a slightly decrease of its intensity [31]. In our present report a peak shift was not observed, however with the aging time the intensity increases 28% as it was above described. The decrease in the intensity in those reports was attributed to the precipitation of the Cu-NPs in both solvents, while the no significant shift was related to the encapsulation of the metal core by a carbon shell, as is supported here. The apparent contradictions observed between the decrease in the intensity with the aging time reported in Ref. [17] and the increase reported here, can be attributed to the differences in the ablation time, 5 min here and 30 min in in Ref. [32] (laser fluence and repetition rate frequency were similar), which increases the amount of copper nanoparticles in the last, allowing the possibility of agglomeration and precipitation; behavior not showed up by the as prepared Cu@C-NPs reported here. It is necessary to clarify that for copper–carbon core–shell NPs synthesized by chemical vapor deposition, it was found that the carbon shells capping the copper core [28,29], had a significant effect on the surface-plasmon resonance band and the fluorescence emission, however at least the first behavior was not observed here.

3.2. Characterization of the PL of Cu@C-NPs and C-NPs

With the aim to elucidate the PL response of the samples, we study the emission features of the carbon nanoparticles (C-NPs) based colloidal suspensions and the colloidal Cu@C-NPs suspensions, both in acetone and synthesized under 120 s of ablation time. We propose that during the ablation process of metallic copper in acetone, the laser beam interacts with the acetone molecules (H_3C–C(=O)–CH_3) inducing its breakdown, in such case the ionized carbon species are deposited on the Cu-NPs surface forming a core shell structure Cu@C-NPs. This was probed by focusing the laser beam on pure acetone and then irradiating it during 120 s, finding that the irradiated acetone displays a very weak emission; the recorded intensity was ~3% (not showed) of the total intensity measured in the colloidal Cu@C-NPs suspensions to obtained during 120 s of ablation. The thermal decomposition of solvents during a LASL experiment has been already reported in [31,40]. The formation of carbon shells on nanoparticles synthesized through LASL was recently explained in terms of the thermal decomposition of the organic liquid (toluene or chloroform) in contact with hot inorganic nanoparticles ejected from the bulk target ($LiNbO_3$, Au or Si) [40]. Presumably, this is the mechanism of formation of the carbon shell observed in the Cu@C-NPs reported here, by virtue of the carbon contained in acetone, which is also mentioned in references [30,31], using solvents as acetone and methanol, respectively. In Fig. 3, the PL spectra of colloidal C-NPs (triangles) and Cu@C-NPs (circles) suspensions obtained under the same experimental conditions are showed. Both PL spectra are very similar, indicating that the carbon shell is, as we assumed yet, the responsible for the photoluminescence observed in the Cu@C-NPs suspensions. It is worth mentioning that colloidal Cu-NPs synthesized in water (not showed here) do not showed photoluminescence. As was above described, the carbon shell stabilizes the colloidal Cu@C-NPs in acetone, as the liquid medium when synthesized by the LASL technique, obtaining a photoluminescence colloidal suspension of Cu@C-NPs.

3.3. Effect of the aging time on the PL intensity

Fig. 4 shows the PL spectra (exciting at 369 nm) of the colloidal Cu@C-NPs suspensions obtained at different ablation times. Fig. 4A and B correspond to the measured spectra 0 days and 30 days after its synthesis, respectively. The PL spectrum of acetone (pink line) was also measured and included in Fig. 4A and B for comparison. While the colloidal Cu@C-NPs suspensions, 0 days from the synthesis, show a PL band centered at 433 nm, acetone does not show a significant PL signal. The PL intensity of the colloidal Cu@C-NPs suspensions slightly increases when increasing the ablation time (Fig. 4C).

For the sample aged for 30 days, interesting changes are observed. Fig. 4B show how the original non-well shaped PL emission bands (Fig. 4A) acquire a close-Gaussian shape. The broad emission band ranging from 380 nm to 540 nm is centered at 433 nm and several peaks can be appreciated for all the spectrums without any tendency in the PL intensity as a function of the irradiation time. In a previous report, this behavior in the PL emission of Cu nanoparticles was observed for samples obtained with different laser fluences in the same solvent [16]. However, in that case the band was centered between 424 and 430 nm, with several peaks around it, when exciting with 230 nm, indicating that the origin of the PL emission have different nature in both cases. In the present report the PL response is mainly related with the carbon presence, while in Ref. [16] the PL emissions were attributed to interband transitions occurred in a few nanometers nanoparticles, mostly supported by the size of the nanoparticles, 1–5 nm. When water was used as liquid media (in which no carbon is present), a broad band centered at 397 nm with at least two peaks around it was recorded in samples excited with 355 nm; in that case, the oxidation was presumed to be responsible of the observed

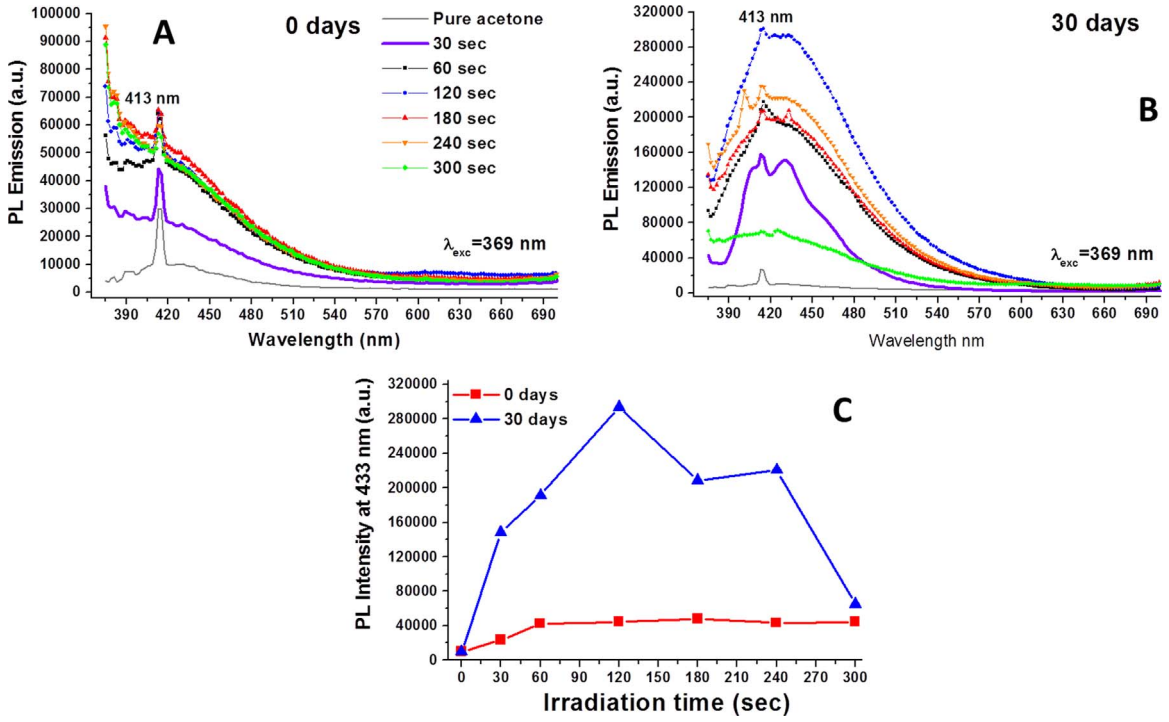

Fig. 4. PL spectra of the Cu@C-NPs suspensions 0 days (A) and 30 days (B) from its synthesis. D - Maximum PL recorded for 433 nm for each irradiation time at the times for A, B and C figures. (For interpretation of the references to color in this figure, the reader is referred to the web version of this article.)

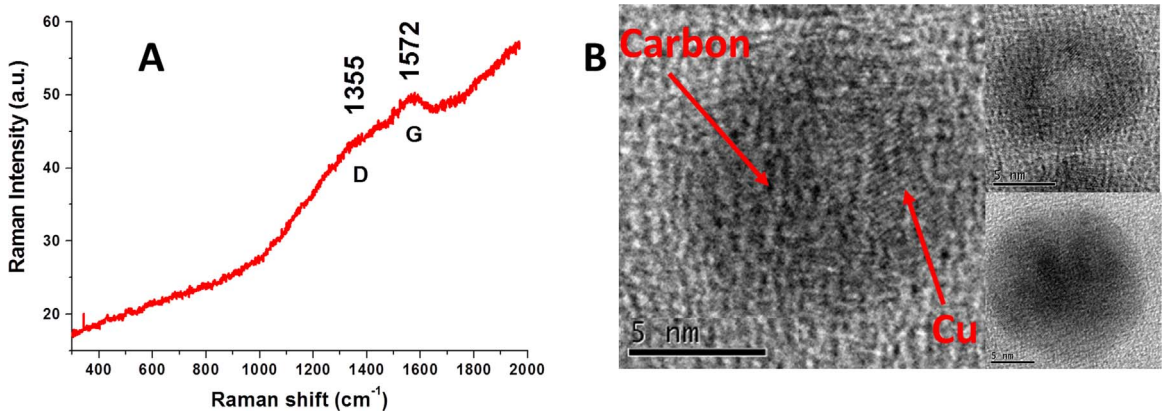

Fig. 5. A - Raman spectrum of the as prepared Cu@C-NPs in which the typical D and G peaks of carbon were identified. B - Typical shape of the Cu@C-NPs in which copper and carbon are identified.

fluorescence. These reports allow pointing out that the multiple peaks forming the PL band reported here can come from different emission traps presents in the Cu@C-NPs.

The maximum value of the PL intensity measured at 433 nm is plotted as a function of the colloidal Cu@C-NPs concentration and shown Fig. 4C for those samples aged during 0 days (red squares) and 30 days (blue triangles). An important increment in the intensity of the emission band is obtained in the sample aged for 30 days. The PL reaches its maximum intensity in the sample synthesized at 120 s of ablation time, representing an increment of 500% with respect to that sample synthesized under same conditions but aged for 0 days. In ref. [16] above discussed, the effect of the laser fluence was analyzed for Cu nanoparticles produced by LASL in the same solvent, the main peak reaches its maximum value at 1.5 J/cm^2, being less for 1, 2, 2.5 and 3 J/cm^2, which is a similar behavior observed here. The presumable explanation is that when increasing the irradiation time or laser fluence, the amount of the produced Cu-NPs or Cu@C-NPs is also increased, in such case the emitted photons due to the excitations are absorbed by the large amount of nanoparticles, which can also occurs with the incident photons, reducing the emission efficiency. In that sense as reported in Ref. [16], 1.5 J/cm^2 optimize the light emission, here it corresponds to 120 s of ablation time. The decrease in the PL intensity of carbon dots obtained by LALS when increasing the ablation time was recently reported by the authors of the present work [38], making feasible the previous supposition. Even when measurements of the carbon shell thickness were no performed in this study, we believe that the previous behavior may be related with a critical thickness of the carbon shell that optimizes the PL emission intensity. Under this argument, if the thickness of the carbon shell is greater than the critical thickness, the PL emission will decrease due to the carbon defects that can be also act as traps for the emitted photons. In order to clarify the dependence of the PL intensity on the thickness of the carbon shell, more studies are required.

3.4. Raman and TEM results

The sample synthesized at 300 s of ablation time was analyzed. The presence of a non-uniform carbon shell on the surface of Cu-NPs to

form Cu@C-NPs was corroborated by TEM and Raman spectroscopy as shown in Fig. 5. Both, TEM and Raman analysis were done with the sample obtained under 300 s of ablation time and 30 days aged after its synthesis. The Raman spectrum in Fig. 5A shows the D and G bands, which, after a fitting of the raw data were identified at 1355 cm^{-1} and 1572 cm^{-1}, respectively, that are assigned to carbon vibration in the carbon shell of the Cu@C-NPs. The preparation of Cu@C-NPs either using chemical routes [23–27] or LASL technique [30,31] has been already reported. Fig. 5B shows TEM images of some Cu@C-NPs, displaying the typical shape and size of the as obtained Cu@C-NPs, showing spheroidal nanoparticles of around 10 nm sizes. Interplanar lines corresponding to a core of copper (Cu) are present and the carbon (C) shell is clear around the copper core. The TEM image is similar to that reported in references [30] or [33], however is clear that more detailed analysis needs to be performed to insight the entire features of the carbon shell (HRTEM or XPS, for example). As was above mentioned hybrid inorganic core–carbon shell nanoparticles based on $LiNbO_3$, Au or Si as core and carbon as shell were have also reported in hydrocarbon liquids such as toluene and chloroform [40], in such case, beside of the reports in references [30,31], it is clear the observed carbon shell on the nanoparticles reported here. It is necessary to indicate that for a better understanding of the carbon shell nature, a more detailed analysis of the carbon shell for each ablation time needs to be done.

4. Conclusions

We reported the use of LASL technique for the facile and fast synthesis of photoluminiscent Cu@C-NPs, proposing that the observed PL emission has its origin in the carbon coating formed during the ablation process in which the carbon species are produced during the thermal decomposition of the liquid acetone in contact with hot copper nanoparticles ejected from the bulk target, are deposited on the Cu-NPs surface forming a copper-core carbon shell structure, called Cu@C-NPs. The PL intensity of the colloidal Cu@C-NPs in acetone was found to be dependent on the ablation time and the aging time after the synthesis. An increment over 500% of the PL intensity was measured in samples synthesized at 120 s of ablation time and aged for 30 days after their synthesis. Absorbance yielded to identify the plasmon resonance typifying the cooper nanostructures, while the presence of carbon was confirmed by microRaman. A more detailed work to determine the carbon nature is required. Even so, we believe that the reported results help to increase the understanding of the formation in one step of Cu@C-based core@shell nanoparticles, and how the presence of the carbon shell impacts on its optical properties; the as prepared nanoparticles could have important application in catalysis and light emission sources.

Acknowledgments

This work was partially supported by SIEA-UAEM under the contract 3885/2015FS. González-Aguilar acknowledges for financial support through the same contract to developed her undergraduate thesis.

References

[1] C.J. Murphy, T.K. Sau, A.M. Gole, C.J. Orendorff, J. Gao, L. Gou, S.E. Hynyadi, T. Li, Anisotropic metal nanoparticles: synthesis, assembly, and optical applications, J. Phys. Chem. 109 (2005) 13857–13870.
[2] G. Oskam, Metal oxide nanoparticles: synthesis, characterization and application, J. Sol-Gel Sci. Tecnol. 37 (2006) 161–164.
[3] X. Lu, C. Wang, Y. Wei, One-dimensional composite nanomaterials: synthesis by electrospinning and their applications, Small 5 (2009) 2349–2370.
[4] K. Grieve, P. Mulvaney, F. Grieser, Synthesis and electronic properties of semiconductor nanoparticles/quantum dots, Curr. Opin. Colloid Interface Sci. 5 (2000) 168–172.
[5] V. Amendola, M. Meneghetti, What controls the composition and the structure of nanomaterials generated by laser ablation in liquid solution?, Phys. Chem. Chem. Phys. 15 (2013) 3027–3046.
[6] C.-H. Yu, K. Tam, E.S.C. Tsang, Chemical methods for preparation of nanoparticles in solution, Handb. Met. Phys. (Met. Nanopart.) 5 (2008) 113–141.
[7] V. Amendola, M. Meneghetti, Laser ablation synthesis in solution and size manipulation of noble metal nanoparticles, Phys. Chem. Chem. Phys. 11 (2009) 3805–3821.
[8] V.K. Sharma, R.A. Yngard, Y. Lin, Silver nanoparticles: green synthesis and their antimicrobial activities, Adv. Colloid Interface Sci. 145 (2009) 83–96.
[9] M. Rodio, R. Brescia, A. Diaspro, R. Intartaglia, Direct surface modification of ligand-free silicon quantum dots prepared by femtosecond laser ablation in deionized water, J. Collid Interface Sci. 465 (2016) 242–248.
[10] K. Bagga, A. Barchanski, R. Intartaglia, S. Dante, R. Marotta, A. Diaspro, C.L. Sajti, F. Brandi, Laser-assisted synthesis of Staphylococcus aureus protein-capped silicon quantum dots as bio-functional nanoprobes, Laser Phys. Lett. 10 (2013) 065603.
[11] T.M. Dung Dang, T.T. Thu Le, E. Fribourg-Blanc, M. Chien Dang, Synthesis and optical properties of copper nanoparticles prepared by a chemical reduction method, Adv. Nat. Sci.: Nanosci. Nanotechnol. 2 (2011) 015009.
[12] Y. Lee, J. Choi, K. Jong Lee, N.E. Stott, D. Kim, Large-scale synthesis of copper nanoparticles by chemically controlled reduction for applications of inkjet-printed electronics, Nanotechnology 19 (2008) 415604.
[13] Q. Darugar, W. Qian, M.A. El-Sayed, M.P. Pileni, Size-dependent ultrafast electronic energy relaxation and enhanced fluorescence of copper nanoparticles, J. Phys. Chem. B 110 (2006) 143–149.
[14] M. Muniz-Miranda, C. Gellini, E. Giorgetti, Surface-enhanced raman scattering from copper nanoparticles obtained by laser ablation, J. Phys. Chem. C 115 (2011) 5021–5027.
[15] M. Muniz Miranda, C. Gellini, A. Simonelli, M. Tiberi, F. Giammanco, E. Giorgetti, Characterization of copper nanoparticles obtained by laser ablation in liquids, Appl. Phys. A Mater. Sci. Process. 110 (2012) 829–833.
[16] D. Dorranian, S.A. Ahmadi Afshar, N. Tahmasebi, A.F. Eskandari, Effect of laser pulse energy on the characteristics of cu nanoparticles produced by laser ablation method in acetone, J. Clust. Sci. 25 (2014) 1147–1156.
[17] R.M. Tilaki, A.I. Zad, S.M. Mahdavi, Size, composition and optical properties of copper nanoparticles prepared by laser ablation in liquids, Appl. Phys. A 88 (2007) 415–419.
[18] H.J. Lee, J. Yong Song, B. Soo Kim, Biological synthesis of copper nanoparticles using Magnolia kobus leaf extract and their antibacterial activity, J. Chem. Technol. Biotechnol. 88 (2013) 1971–1977.
[19] N. Vilar-Vidal, M. Carmen Blanco, M.A. Lopez-Quintela, J. Rivas, C. Serra, Electrochemical synthesis of very stable photoluminescent copper clusters, J. Phys. Chem. C 114 (2010) 15924–15930.
[20] G. Saito, S. Hosokai, M. Tsubota, T. Akiyama, Synthesis of copper/copper oxide nanoparticles by solution plasma, J. Appl. Phys. 110 (2011) 023302.
[21] Syed Saif Hasan, Sanjay Singh, Parikh, Y. Rasesh, Dharne, S. Mahesh, Patole, S. Milind, B.L.V. Prasad, Shouche, S. Yogesh, Bacterial synthesis of copper/copper oxide nanoparticles, J. Nanosci. Nanotechnol. 8 (2008) 3191–3196.
[22] B. Sharma, M.K. Rabinal, Ambient synthesis and optoelectronic properties of copper iodide semiconductor nanoparticles, J. Alloy. Compd. 556 (2013) 198–202.
[23] E.K. Athanassiou, R.N. Grass, W.J. Stark, Large-scale production of carbon-coated copper nanoparticles for sensor applications, Nanotechnology 17 (2006) 1668–1673.
[24] J. Lia, C.-Y. Liu, Carbon-coated copper nanoparticles: synthesis, characterization and optical properties, New J. Chem. 33 (2009) 1474–1477.
[25] N. Luo, X.J. Li, K.X. Liu, L.M. Ye, T.W. Chen, Preparation of carbon-coated copper nanoparticles by detonation decomposition of copper ion doped sol–gel explosive precursors, J. Nanopart. Res. 15 (2013) 1614.
[26] D.S. Jacob, I. Genish, L. Klein, A. Gedanken, Carbon-coated core shell structured copper and nickel nanoparticles synthesized in an ionic liquid, J. Phys. Chem. B 110 (2006) 1711–1714.
[27] J. Zhai, X. Tao, Y. Pu, X.-F. Zeng, J.-F. Chen, Controllable synthesis and characterization of novel copper–carbon core–shell structured nanoparticles, Mater. Res. Bull. 46 (2011) 865–870.
[28] L. Ma, B. Yu, S. Wang, G. Su, H. Huang, H. Chen, Y. He, J. Zou, Controlled synthesis and optical properties of Cu/C core/shell nanoparticles, Nanopart. Res. 16 (2014) 2545.
[29] J. Zhai, X. Tao, Y. Pu, X.F. Zeng, J.F. Chen, Controllable synthesis and characterization of novel copper–carbon core–shell structured nanoparticles, Mater. Res. Bull. 46 (2011) 865–870.
[30] P.V. Kazakevich, A.V. Simakin, V.V. Voronov, G.A. Shafeev, D. Starikov, A. Bensaoula, Formation of core-shell nanoparticles by laser ablation of copper and brass in liquids, Solid State Phenom. 106 (2005) 23–26.
[31] P. Liu, H. Wang, X. Li, M. Rui, H. Zeng, Localized surface plasmon resonance of Cu nanoparticles by laser ablation in liquid media, RSC Adv. 5 (2015) 79738–79745.
[32] A.K. Schaper, H. Hou, A. greiner, R. Schneider, F. Phillipp, Copper nanoparticles encapsulated in multi-shell carbon cages, Appl. Phys. A 78 (2004) 73–77.
[33] S. Wang, X. Huang, Y. He, H. Huang, Y. Wu, L. Hou, X. Liu, T. Yang, J. Zou, B. Huang, Synthesis, growth mechanism and thermal stability of copper nanoparticles encapsulated by multi-layer graphene, Carbon 50 (2012) 2119–2125.
[34] N.A. Luechinger, E.K. Athanassiou, W.J. Stark, Graphene-stabilized copper nanoparticles as an air-stable substitute for silver and gold in low-cost ink-jet printable electronics, Nanotechnology 19 (2008) 445201.
[35] L. D'Urso, G. Grasso, E. Messina, C. Bongiorno, V. Scuderi, S. Scalese, O. Puglisi, G. Spoto, G. Compagnini, Role of linear carbon chains in the aggregation of copper, silver, and gold nanoparticles, J. Phys. Chem. C 114 (2010) 907–915.
[36] K.H. Müller, M. Motskin, A.J. Philpott, A.F. Routh, C.M. Shanahan, M.J. Duer,

J.N. Skepper, The effect of particle agglomeration on the formation of a surface-connected compartment induced by hydroxyapatite nanoparticles in human monocyte-derived macrophages, Biomaterials 35 (2014) 1074–1088.
[37] D. Reyes-Contreras, M. Camacho-López, M.A. Camacho-López, S. Camacho-López, René I. Rodríguez Beltrán, M. Mayorga, Influence of the per pulse laser fluence on the optical properties of carbon nanoparticles synthesized by laser ablation of solids in liquids, Opt. Laser Technol. 74 (2015) 48–52.
[38] D. Reyes, M. Camacho, M.A. Camacho, M. Mayorga, D. Weathers, G. Salamo, Z. Wang, A. Neogi, Laser ablated carbon nanodots for light emission, Nanoscale Res. Lett. 11 (2016) 424–435.
[39] C. Noguez, Surface plasmons on metal nanoparticles: the influence of shape and physical environment, J. Phys. Chem. C 111 (2007) 3806–3819.
[40] R. García-Calzada, M. Rodio, K. Bagga, R. Intartaglia, P. Bianchini, V.S. Chirvony, J.P. Martínez-Pastor, Facile laser-assisted synthesis of inorganic nanoparticles covered by a carbon shell with tunable luminescent, RSC Adv. 5 (2015) 50604–50610.